CONFIDENTIAL
CLASSIFICATION CANCELLED
AUTHORITY NASA TECHNICAL PUBLICATIONS ANNOUNCEMENTS NO. 33 DATE 12-6-60 BY
UNAVAILABLE

Copy /
RM SL55D25

NACA

RESEARCH MEMORANDUM

for the

Bureau of Aeronautics, Department of the Navy

WIND-TUNNEL INVESTIGATION AT LOW SPEED OF THE YAWING, PITCHING, AND STATIC STABILITY CHARACTERISTICS OF A 1/10-SCALE MODEL OF THE GRUMMAN F9F-9 AIRPLANE

TED No. NACA AD 3109

By Walter D. Wolhart and David F. Thomas, Jr.

Langley Aeronautical Laboratory
Langley Field, Va.

CLASSIFIED DOCUMENT

This material contains information affecting the National Defense of the United States within the meaning of the espionage laws, Title 18, U.S.C., Secs. 793 and 794, the transmission or revelation of which in any manner to an unauthorized person is prohibited by law.

NATIONAL ADVISORY COMMITTEE
FOR AERONAUTICS

WASHINGTON

APR 13 1955

FILE COPY
To be returned to the files of the National Advisory Committee for Aeronautics Washington, D. C.

16

CLASSIFICATION CANCELLED
AUTHORITY NASA TECHNICAL PUBLICATIONS ANNOUNCEMENTS NO. DATE BY
CONFIDENTIAL

CLASSIFICATION CANCELLED
AUTHORITY NASA TECHNICAL PUBLICATIONS
ANNOUNCEMENTS NO. DATE BY

NATIONAL ADVISORY COMMITTEE FOR AERONAUTICS

RESEARCH MEMORANDUM

for the

Bureau of Aeronautics, Department of the Navy

WIND-TUNNEL INVESTIGATION AT LOW SPEED OF THE YAWING, PITCHING, AND STATIC STABILITY CHARACTERISTICS OF A 1/10-SCALE MODEL OF THE GRUMMAN F9F-9 AIRPLANE

TED No. NACA AD 3109

By Walter D. Wolhart and David F. Thomas, Jr.

SUMMARY

An experimental investigation has been made in the Langley stability tunnel to determine the low-speed yawing, pitching, and static stability characteristics of a 1/10-scale model of the Grumman F9F-9 airplane. Tests were made to determine the effects of duct-entrance-fairing plugs on the static lateral and longitudinal stability characteristics of the complete model in the clean condition. The remaining tests were concerned with determining tail contributions as well as the effect of duct-entrance-fairing plugs, slats, flaps, and landing gear on the yawing and pitching stability derivatives. These data are presented without analysis in order to expedite distribution.

INTRODUCTION

Previous investigations have indicated that reliable prediction of dynamic flight characteristics over a wide angle-of-attack range requires more accurate estimates of the various aerodynamic parameters than are possible with the use of available procedures. (See refs. 1 and 2, for example.)

CLASSIFICATION CANCELLED
AUTHORITY NASA TECHNICAL PUBLICATIONS
ANNOUNCEMENTS NO. DATE BY

The purpose of the present investigation was to determine the yawing and pitching stability derivatives of various clean and landing configurations of a 1/10-scale model of the Grumman F9F-9 airplane. This part of the investigation included determining the tail contributions as well as the effects of slats, flaps, and landing gear. The static lateral and longitudinal stability characteristics of a basic clean configuration were determined in order to provide a basis of comparison with large-scale results from other sources as an aid in evaluating the results of this investigation when applied to the full-scale airplane.

These tests were made at the request of the Bureau of Aeronautics, Department of the Navy, to aid in the development of the Grumman F9F-9 airplane.

SYMBOLS

The data presented herein are in the form of standard NACA coefficients of forces and moments which are referred to the stability system of axes with the origin at the center of gravity. All coefficients are based on the basic wing which has an area of 2.502 square feet as compared with an area of 2.548 square feet for the basic wing plus the leading-edge extension. The positive direction of forces, moments, and angular displacements is shown in figure 1. The coefficients and symbols are defined as follows:

L	lift, lb
D	drag, lb
Y	lateral force, lb
M	pitching moment, ft-lb
L'	rolling moment, ft-lb
N	yawing moment, ft-lb
b	span, ft
S	area, sq ft
c	chord, measured parallel to plane of symmetry, ft
$\bar{c}$	mean aerodynamic chord, $\frac{2}{S}\int_0^{b/2} c^2 dy$, ft

y	spanwise distance from and perpendicular to plane of symmetry, ft
q_o	free-stream dynamic pressure, $\rho V^2/2$, lb/sq ft
V	free-stream velocity, ft/sec
ρ	mass density of air, slugs/cu ft
α	angle of attack of fuselage reference line, deg
θ	angle of pitch, deg
γ	flight-path angle, deg
ϕ	angle of roll, deg
β	angle of sideslip, deg
ψ	angle of yaw, deg
C_L	lift coefficient, L/q_oS_w
C_D	drag coefficient, D/q_oS_w
C_Y	lateral-force coefficient, Y/q_oS_w
C_m	pitching-moment coefficient, $M/q_oS_w\bar{c}_w$
C_l	rolling-moment coefficient, $L'/q_oS_wb_w$
C_n	yawing-moment coefficient, $N/q_oS_wb_w$
$rb/2V$	yawing-angular-velocity parameter, radians
r	yawing angular velocity, $d\psi/dt$, radians/sec
$q\bar{c}/2V$	pitching-angular-velocity parameter, radians
q	pitching angular velocity, $d\theta/dt$, radians/sec

$$C_{Y_\beta} = \frac{\partial C_Y}{\partial \beta}$$

$$C_{l_\beta} = \frac{\partial C_l}{\partial \beta}$$

$$C_{n_\beta} = \frac{\partial C_n}{\partial \beta}$$

$$C_{Y_r} = \frac{\partial C_Y}{\partial \frac{rb}{2V}}$$

$$C_{n_r} = \frac{\partial C_n}{\partial \frac{rb}{2V}}$$

$$C_{l_r} = \frac{\partial C_l}{\partial \frac{rb}{2V}}$$

$$C_{L_q} = \frac{\partial C_L}{\partial \frac{q\bar{c}}{2V}}$$

$$C_{D_q} = \frac{\partial C_D}{\partial \frac{q\bar{c}}{2V}}$$

$$C_{m_q} = \frac{\partial C_m}{\partial \frac{q\bar{c}}{2V}}$$

$\Delta C_{Y_r}, \Delta C_{l_r}, \Delta C_{n_r}$ tare increments due to support strut (to be substracted from basic data)

Subscripts:

w wing

L left

R right

For convenience, the model components are denoted by the following symbols:

W wing

B fuselage

V	vertical tail
H	horizontal tail (used with subscript 0 or -10 to denote horizontal-tail incidence)
Z	wing fences
P	duct-entrance-fairing plugs
G	landing gear extended
G'	landing gear extended, nose-gear doors off
F	flaps deflected (used with subscripts 20, 30, or 40 to denote flap deflection in degrees with respect to wing chord line)
S	slats extended
δ	flaperon deflected (used with superscript 5 to denote flaperon deflection in degrees with respect to local upper surface of wing)

APPARATUS AND MODEL

The tests of the present investigation were made in the 6- by 6-foot curved-flow test section of the Langley stability tunnel in which curved flight is simulated by curving the airstream about a stationary model (ref. 3). Forces and moments on the model were obtained with the model mounted on a single strut support which was in turn fastened to a conventional six-component balance system.

The model used in this investigation was a 1/10-scale model of the Grumman F9F-9 airplane and was supplied to the NACA by the Grumman Aircraft Engineering Corporation. Pertinent geometric characteristics of the model are given in figure 2 and table I. Lateral control on this airplane is provided by flap-type spoiler controls called flaperons (see fig. 2(b)). The left and right flaperons are deflected independently of one another to give left and right rolls, respectively. A symmetrical flaperon deflection of 5°, δ^5_{LR}, corresponds to the neutral flaperon position for all flaps-extended configurations. Photographs of the model are presented in figures 3 and 4. No provisions were made for internal flow; however, removable duct-entrance-fairing plugs were provided so that any interference effects from this area could be determined.

TESTS

All the tests were made at a dynamic pressure of 24.9 pounds per square foot which corresponds to a Mach number of about 0.13 and a Reynolds number of 0.756×10^6 based on the wing mean aerodynamic chord of 0.82 foot. The angle-of-attack range for all tests was from approximately -4° to 20°. The test variables are summarized in the following table:

Test	β, deg	$rb/2V$, radians	$q\bar{c}/2V$, radians
Static longitudinal	0	0	0
Static lateral	± 5	0	0
Yawing	0	0, -.0329, -.0696, -.0917	0
Pitching	0	0	0, .0085, .0180, .0238

CORRECTIONS

Approximate corrections for jet-boundary effects were applied to the angle of attack and drag coefficient by the methods of reference 4. Horizontal-tail-on pitching-moment coefficients were corrected by the methods of reference 5. Blockage corrections were determined by the methods of reference 6 and were applied to the drag coefficient and the dynamic pressure. These data are not corrected for the effects of the support strut since these effects were determined for only the yawing derivatives of the complete landing configuration. These tares are presented and, if applied, are to be substracted from the basic data.

PRESENTATION OF RESULTS

The static lateral and longitudinal stability characteristics are presented in figures 5 and 6, the yawing stability characteristics are presented in figures 7 to 11, and the pitching stability characteristics are presented in figures 12 and 13. For convenience in locating desired information, a summary of the configurations investigated as well as the

figures that give data for these configurations is given in table II. These data are presented without analysis in order to expedite distribution.

Langley Aeronautical Laboratory,
National Advisory Committee for Aeronautics,
Langley Field, Va., March 31, 1955.

Walter D. Wolhart
Aeronautical Research Scientist

David F. Thomas, Jr.
Aeronautical Research Scientist

Approved: Thomas A. Harris

Thomas A. Harris
Chief of Stability Research Division

sam

REFERENCES

1. Jaquet, Byron M., and Fletcher, H. S.: Lateral Oscillatory Characteristics of the Republic F-91 Airplane Calculated by Using Low-Speed Experimental Static and Rotary Derivatives. NACA RM L53G01, 1953.

2. Campbell, John P., and McKinney, Marion O.: Summary of Methods for Calculating Dynamic Lateral Stability and Response and for Estimating Lateral Stability Derivatives. NACA Rep. 1098, 1952. (Supersedes NACA TN 2409.)

3. Bird, John D., Jaquet, Byron M., and Cowan, John W.: Effect of Fuselage and Tail Surfaces on Low-Speed Yawing Characteristics of a Swept-Wing Model As Determined in Curved-Flow Test Section of the Langley Stability Tunnel. NACA TN 2483, 1951. (Supersedes NACA RM L8G13.)

4. Silverstein, Abe, and White, James A.: Wind-Tunnel Interference With Particular Reference to Off-Center Positions of the Wing and to the Downwash at the Tail. NACA Rep. 547, 1936.

5. Gillis, Clarence L., Polhamus, Edward C., and Gray, Joseph L., Jr.: Charts for Determining Jet-Boundary Corrections for Complete Models in 7- by 10-Foot Closed Rectangular Wind Tunnels. NACA WR L-123, 1945. (Formerly NACA ARR L5G31.)

6. Herriot, John G.: Blockage Corrections for Three-Dimensional-Flow Closed-Throat Wind Tunnels, With Consideration of the Effect of Compressibility. NACA Rep. 995, 1950. (Supersedes NACA RM A7B28.)

TABLE I.- GEOMETRIC CHARACTERISTICS OF 1/10-SCALE MODEL OF THE GRUMMAN F9F-9 AIRPLANE

Wing (does not include leading-edge extension):	
Aspect ratio	4.00
Taper ratio	0.50
Quarter-chord sweep angle, deg	35.00
Dihedral angle, deg	-2.50
Airfoil section at root	Modified NACA 65A006
Airfoil section at tip	Modified NACA 65A004
Root chord, ft	1.053
Tip chord, ft	0.526
Area, sq ft	2.502
Span, ft	3.165
Mean aerodynamic chord, ft	0.820
Horizontal tail:	
Aspect ratio	3.50
Taper ratio	0.40
Quarter-chord sweep angle, deg	35.00
Airfoil section at root	NACA 65A006
Airfoil section at tip	NACA 65A004
Root chord (on fuselage reference line), ft	0.619
Tip chord, ft	0.248
Area, sq ft	0.655
Span, ft	1.519
Mean aerodynamic chord, ft	0.460
Tail length (distance from center of gravity to $\bar{c}/4$ of tail), ft	1.26
Vertical tail:	
Aspect ratio	1.50
Taper ratio	0.18
Quarter-chord sweep angle, deg	44.45
Airfoil section at root	NACA 65A006
Airfoil section at tip	NACA 65A006
Root chord (measured 2.70 in. above fuselage reference line), ft	0.875
Tip chord, ft	0.155
Area, sq ft	0.479
Span (measured from 2.70 in. above fuselage reference line), ft	0.775
Tail length (distance from center of gravity to $\bar{c}/4$ of tail), ft	1.234

TABLE II.- SUMMARY OF MODEL CONFIGURATIONS TESTED AND DATA PRESENTED

Model configuration	Data	Figure
$WBZVH_0$ $WBZPVH_0$	Effect of duct-entrance-fairing plugs on clean configuration; C_L, C_D, and C_m plotted against α	5
$WBZVH_0$ $WBZPVH_0$	Effect of duct-entrance-fairing plugs on clean configuration; C_{Y_β}, C_{n_β}, and C_{l_β} plotted against α	6
$WBZVH_0$ $WBZPVH_0$ $WBZPVH_0G$	Effect of duct-entrance-fairing plugs and landing gear on clean configuration; C_{Y_r}, C_{n_r}, and C_{l_r} plotted against α	7
$WBZPVH_0$ $WBZP$ $WBZPF_{30}S\delta^5_{LR}$ $WBZPVH_{-10}F_{30}S\delta^5_{LR}$	Horizontal-tail–vertical-tail contribution for clean and landing configurations; C_{Y_r}, C_{n_r}, and C_{l_r} plotted against α	8
$WBZPVH_0G$ $WBZPVH_{-10}F_{20}S\delta^5_{LR}G$ $WBZPVH_{-10}F_{30}S\delta^5_{LR}G$ $WBZPVH_{-10}F_{40}S\delta^5_{LR}G$	Effect of flap deflection on landing configurations; C_{Y_r}, C_{n_r}, and C_{l_r} plotted against α	9
$WBZPVH_{-10}F_{30}S\delta^5_{LR}$ $WBZPVH_{-10}F_{30}S\delta^5_{LR}G$ $WBZPVH_{-10}F_{30}S\delta^5_{LR}G'$	Effect of landing gear and nose-gear doors on landing configuration; C_{Y_r} C_{n_r}, and C_{l_r} plotted against α	10
$WBZPVH_{-10}F_{30}S\delta^5_{LR}G$	Support-strut tare increments for landing configuration; ΔC_{Y_r}, ΔC_{n_r}, and ΔC_{l_r} plotted against α	11
$WBZPV$ $WBZVH_0$ $WBZPVH_0$ $WBZPVH_0G$	Horizontal-tail contribution and the effect of duct-entrance-fairing plugs and landing gear on clean configuration; C_{L_q}, C_{D_q}, and C_{m_q} plotted against α	12
$WBZPVF_{30}S\delta^5_{LR}$ $WBZPVH_{-10}F_{30}S\delta^5_{LR}$ $WBZPVH_{-10}F_{30}S\delta^5_{LR}G$	Horizontal-tail contribution and the effect of landing gear on landing configuration; C_{L_q}, C_{D_q}, and C_{m_q} plotted against α	13

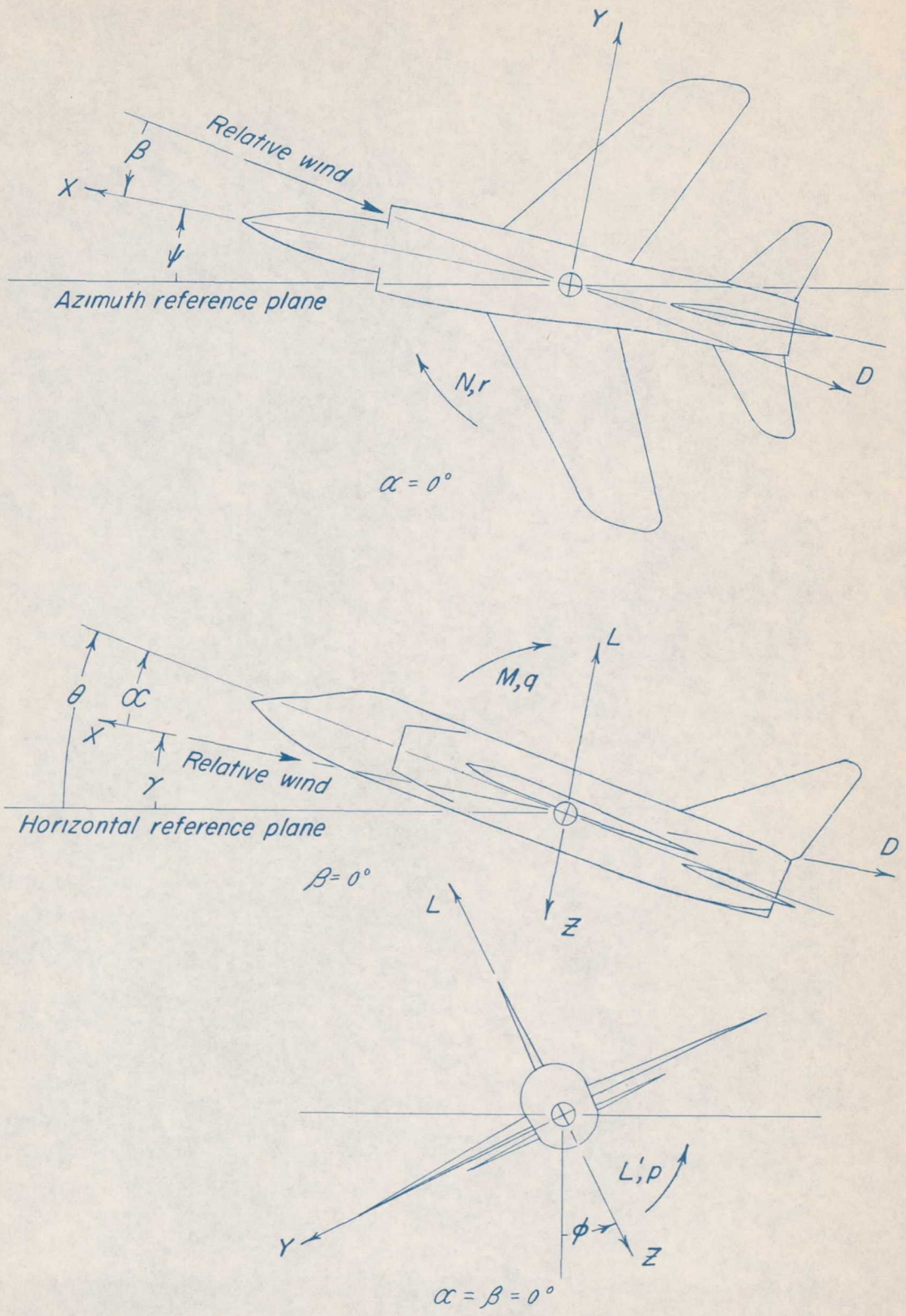

Figure 1.- Stability system of axes. Arrows indicate positive direction of forces, moments, angular displacements, and angular velocities.

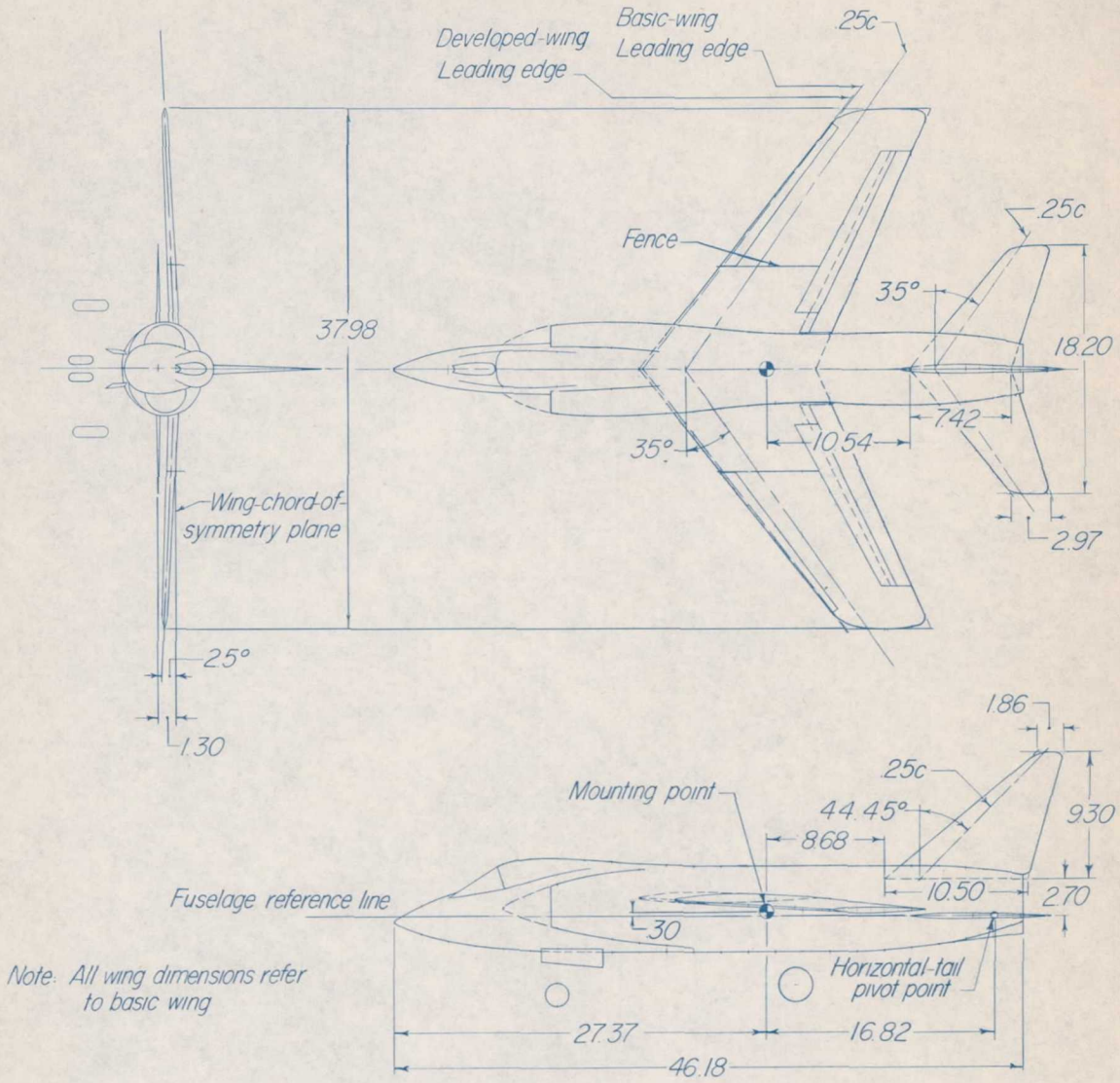

(a) General arrangement.

Figure 2.- Geometric characteristics of 1/10-scale model of the Grumman F9F-9 airplane. All dimensions in inches.

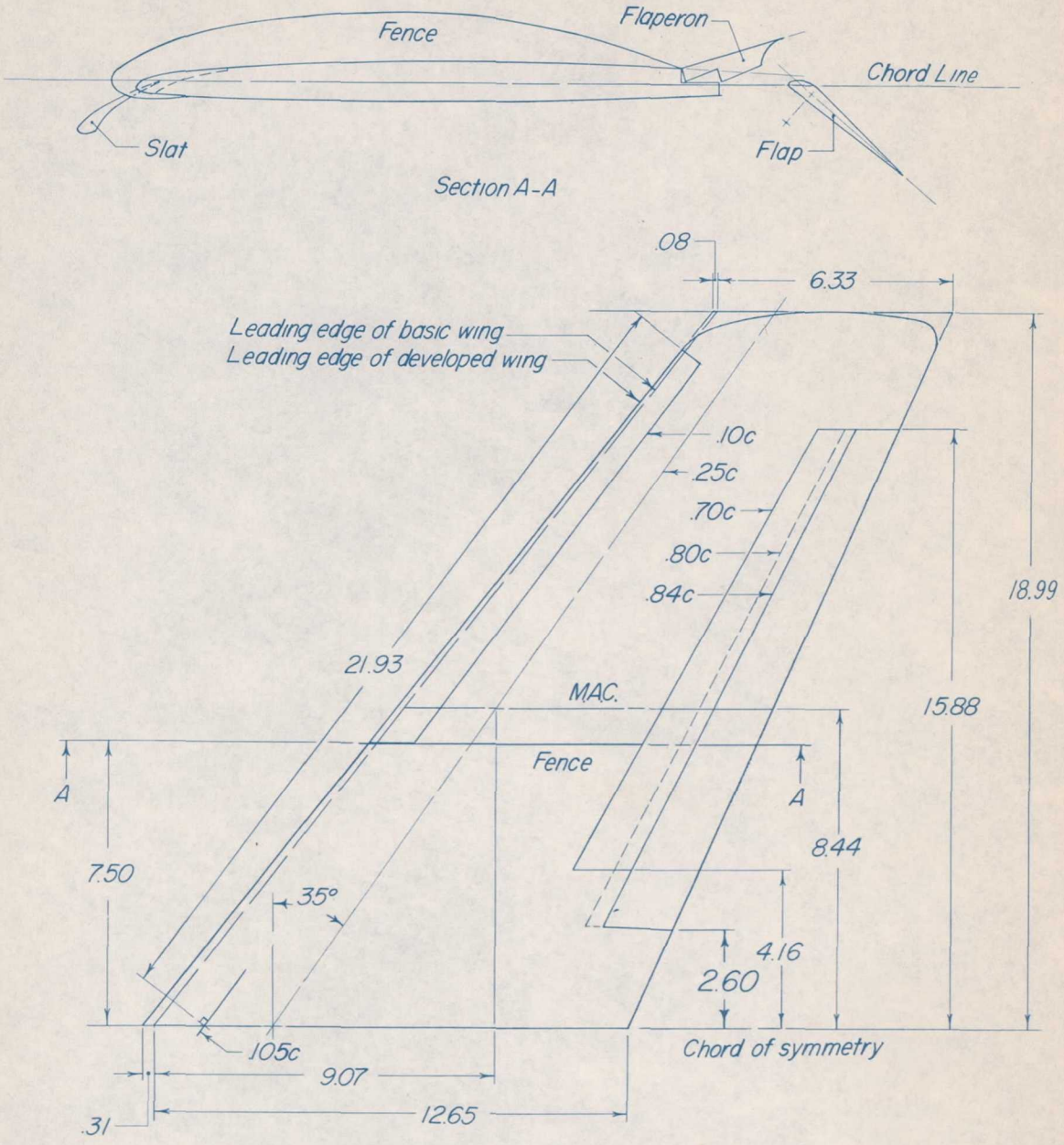

(b) Details of fence, slat, flaps, and flaperon.

Figure 2.- Concluded.

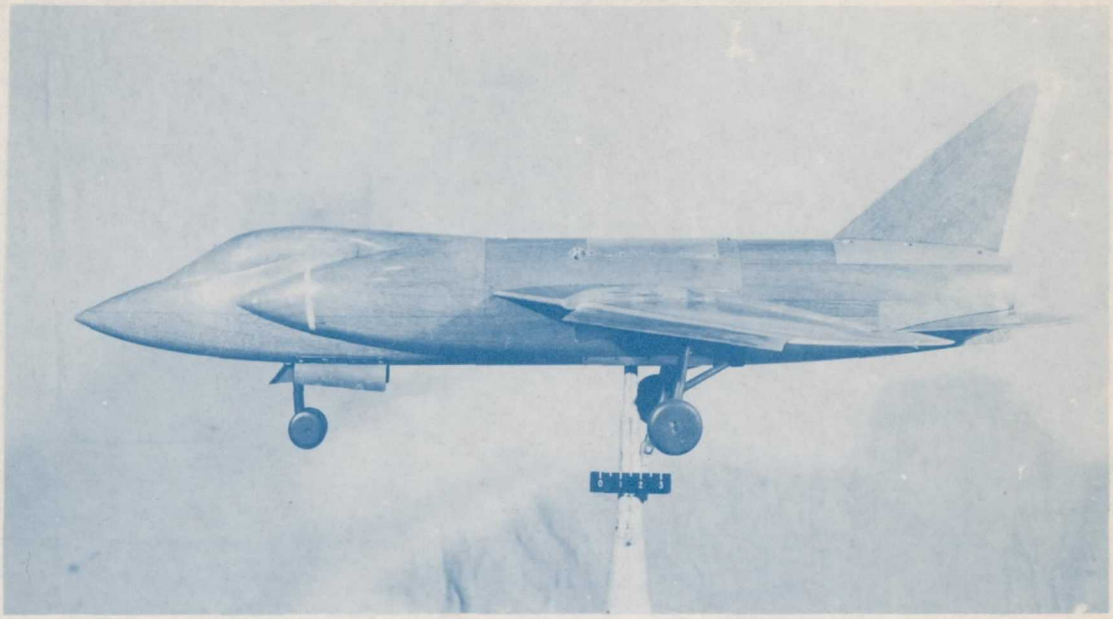

L-87752

(a) Side view of $WBZPVH_{-10}F_{30}S\delta^{5}_{LR}G$ landing configuration.

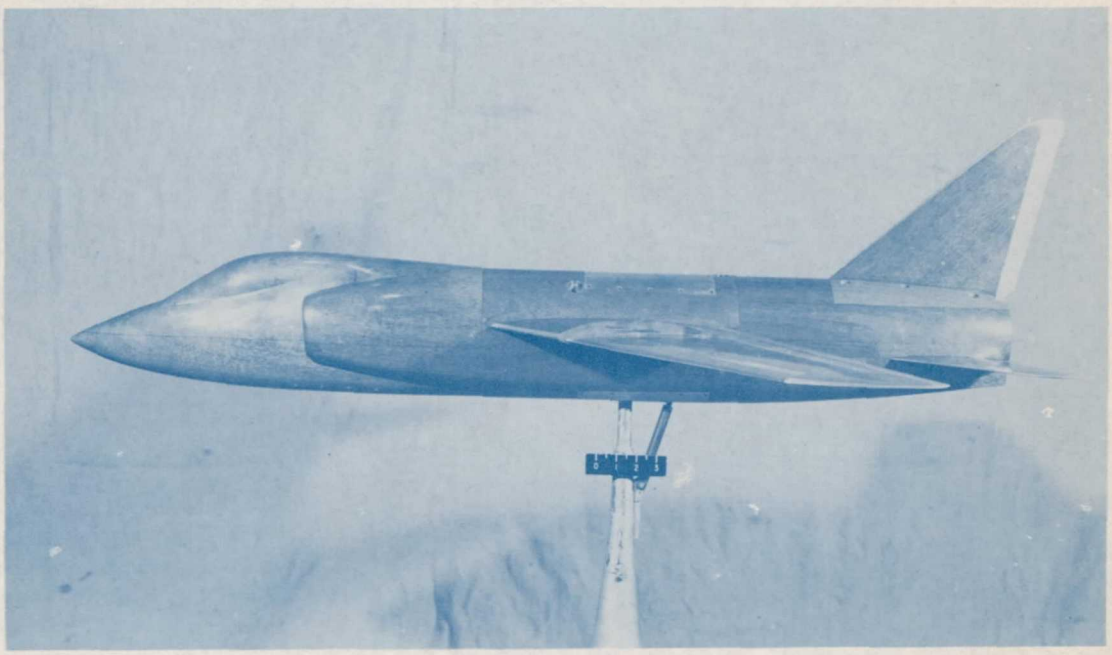

(b) Side view of $WBZVH_{0}$ clean configuration. L-87753

Figure 3.- Photographs of 1/10-scale model of the Grumman F9F-9 airplane mounted on model support pedestal.

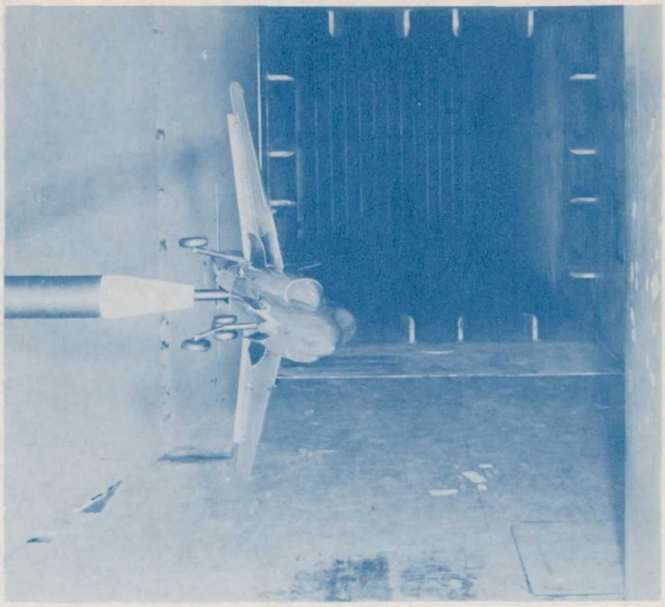

L-87254

(a) Front view of $WBZPVH_{-10}F_{30}S\delta^{5}_{LR}G$ landing configuration.

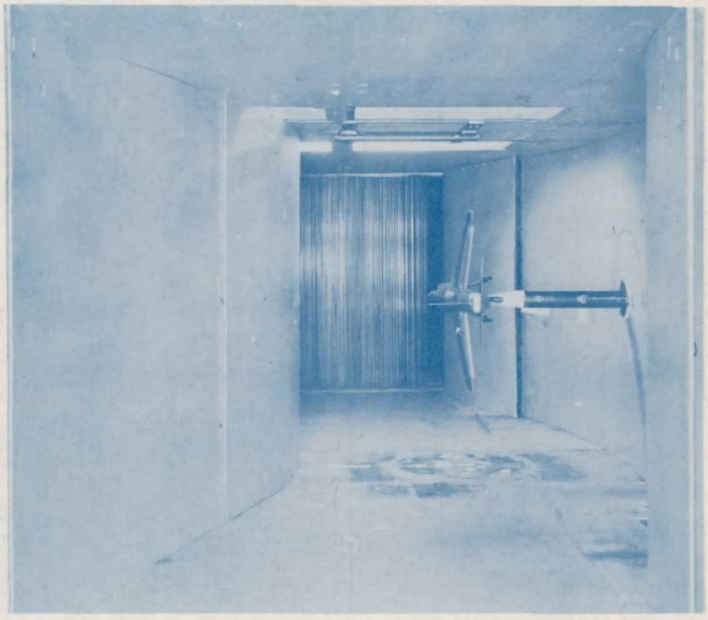

L-87253

(b) Rear view of $WBZPVH_{-10}F_{30}S\delta^{5}_{LR}G$ landing configuration.

Figure 4.- Photographs of 1/10-scale model of the Grumman F9F-9 airplane mounted in the 6- by 6-foot curved-flow test section of the Langley stability tunnel. Pitching-flow test setup.

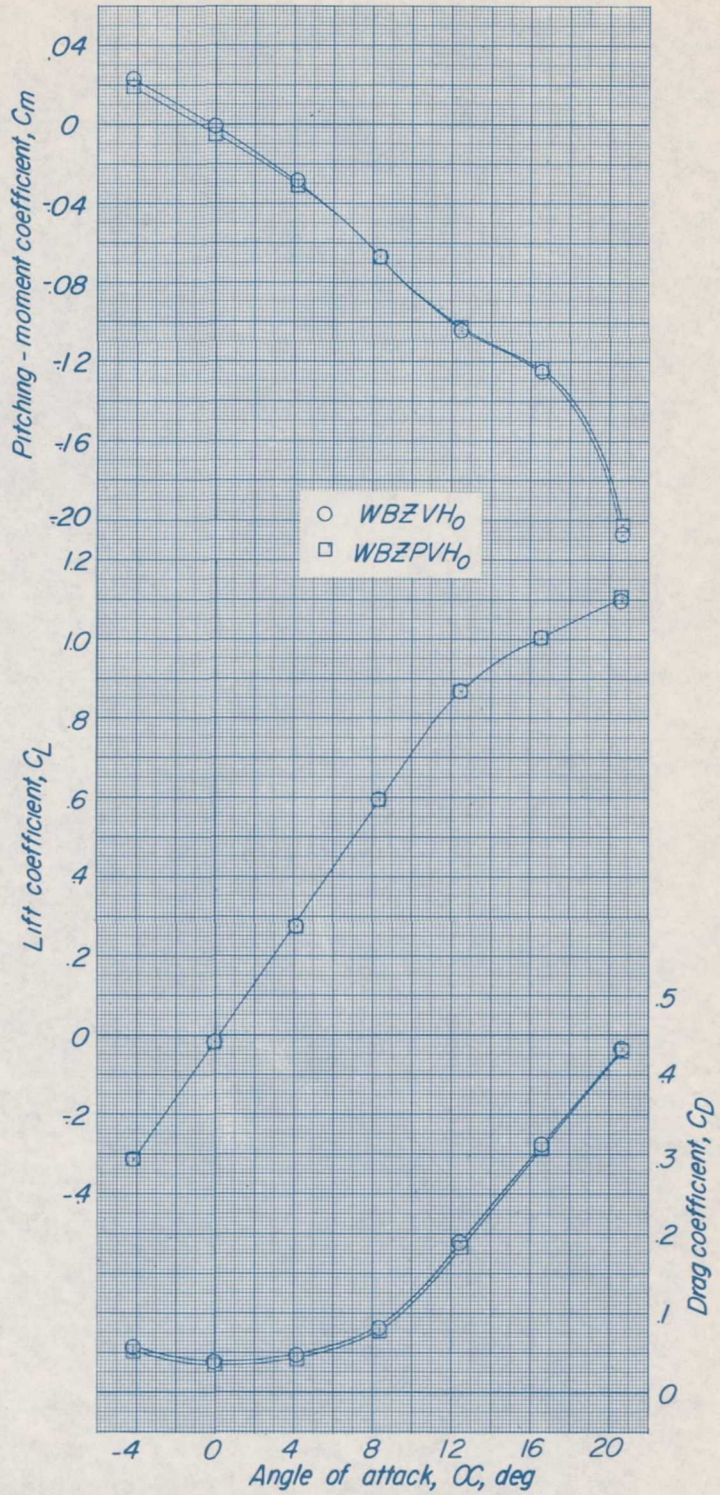

Figure 5.- Effect of duct-entrance-fairing plugs on the static longitudinal stability characteristics. Slats, flaps, flaperons, and landing gear retracted.

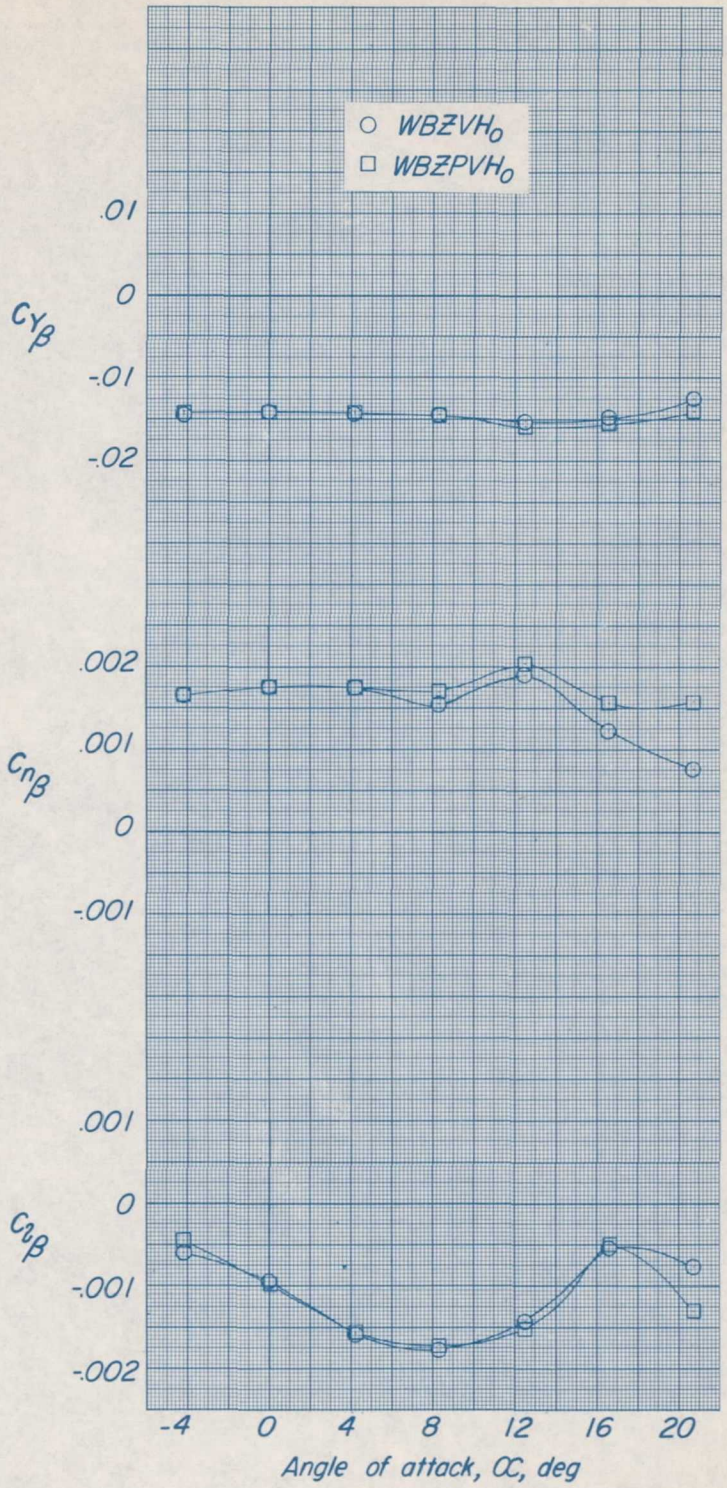

Figure 6.- Effect of duct-entrance-fairing plugs on the static lateral stability characteristics. Slats, flaps, flaperons, and landing gear retracted.

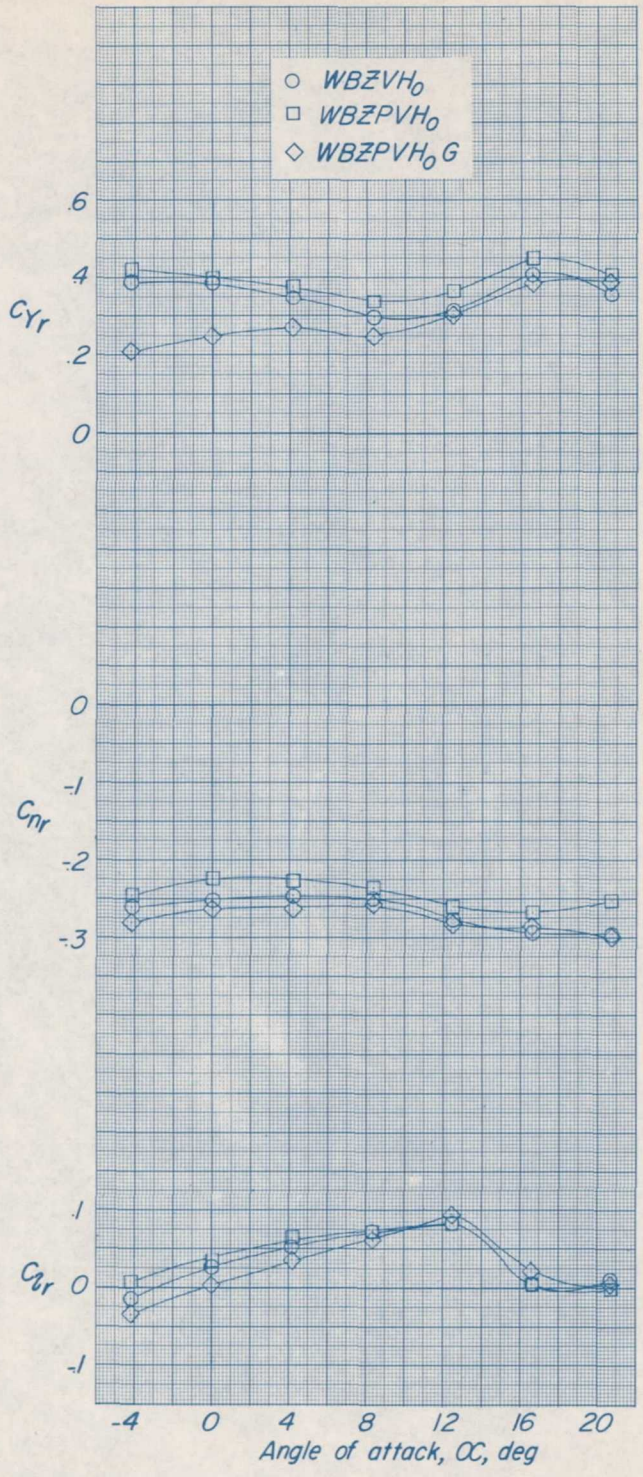

Figure 7.- Effect of duct-entrance-fairing plugs and landing gear on the yawing stability characteristics. Slats, flaps, and flaperons retracted.

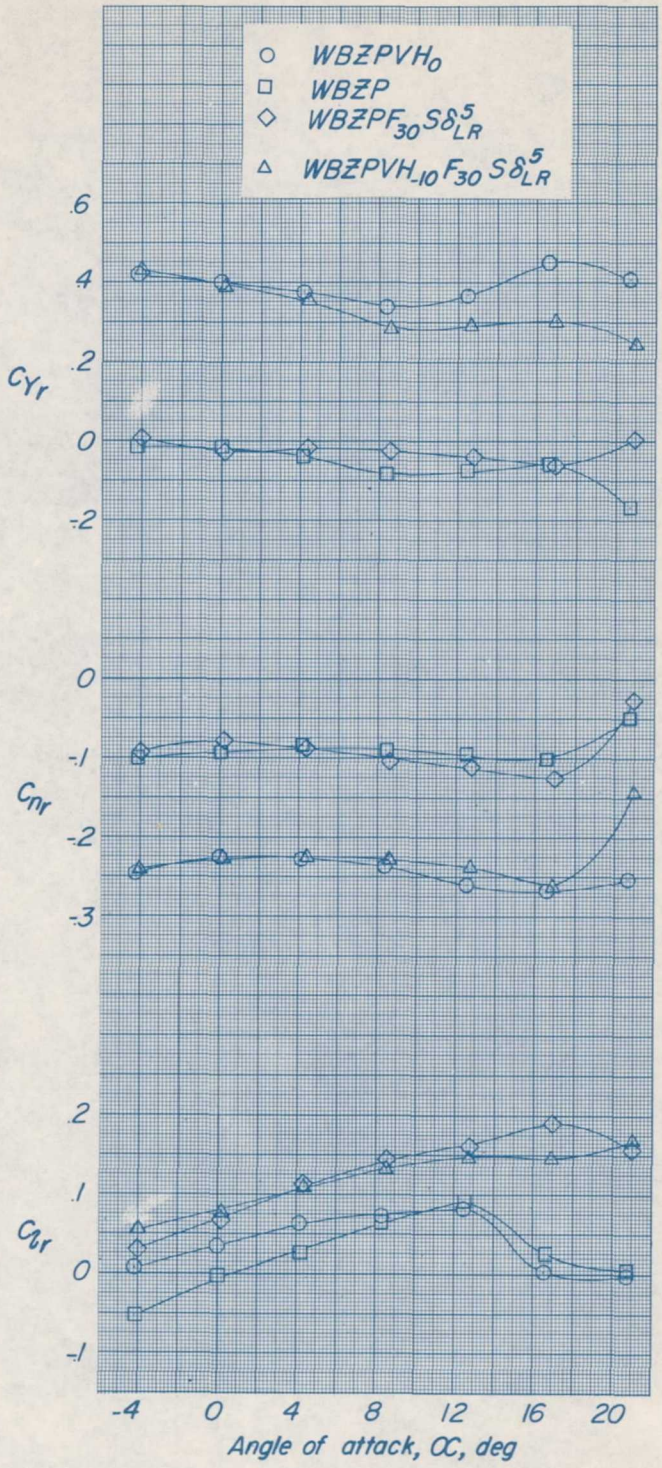

Figure 8.- Horizontal-tail—vertical-tail contribution and the effect of slats, flaps, and flaperons on the yawing stability characteristics. Landing gear retracted.

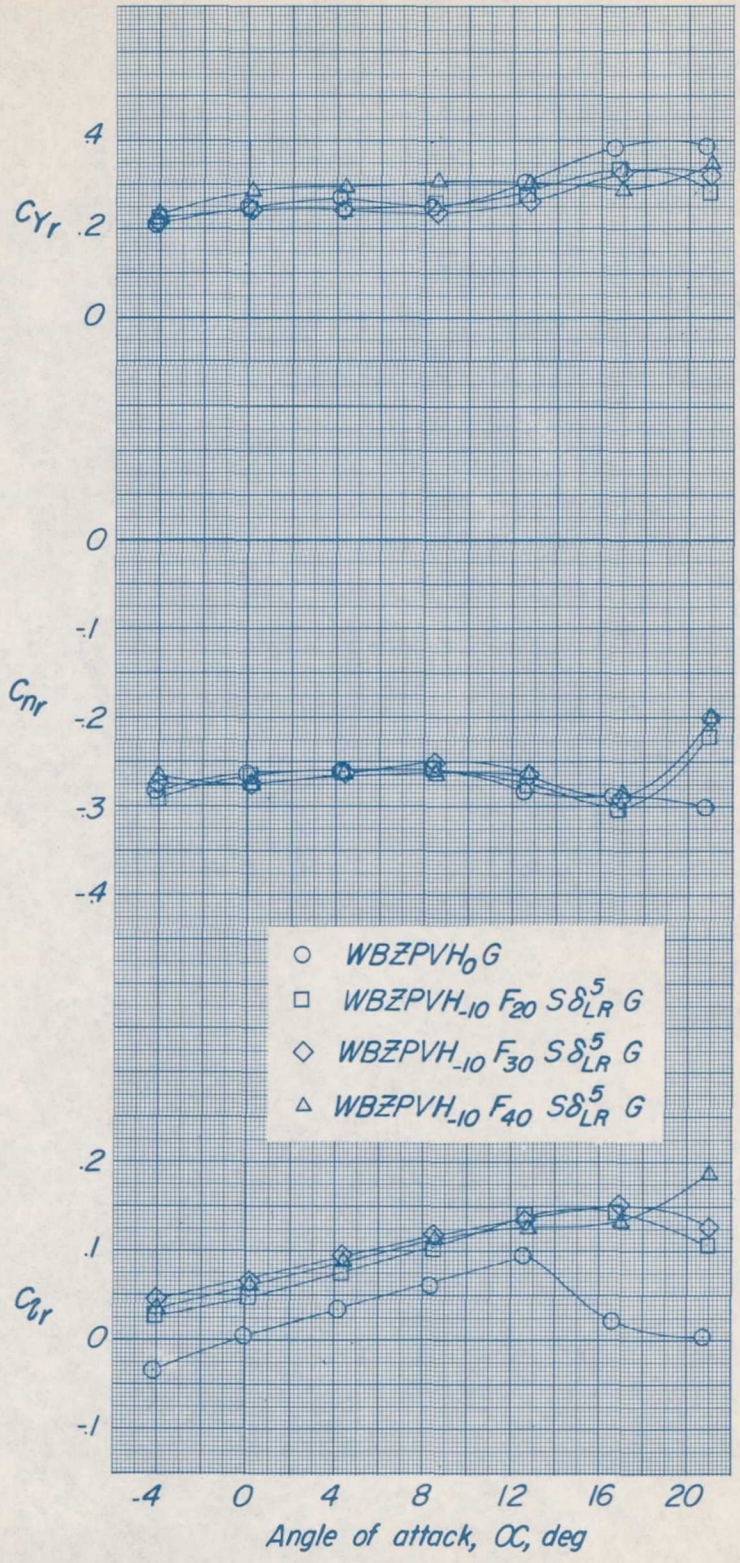

Figure 9.- Effect of slats, flaps, and flaperons on the yawing stability characteristics. Landing gear extended.

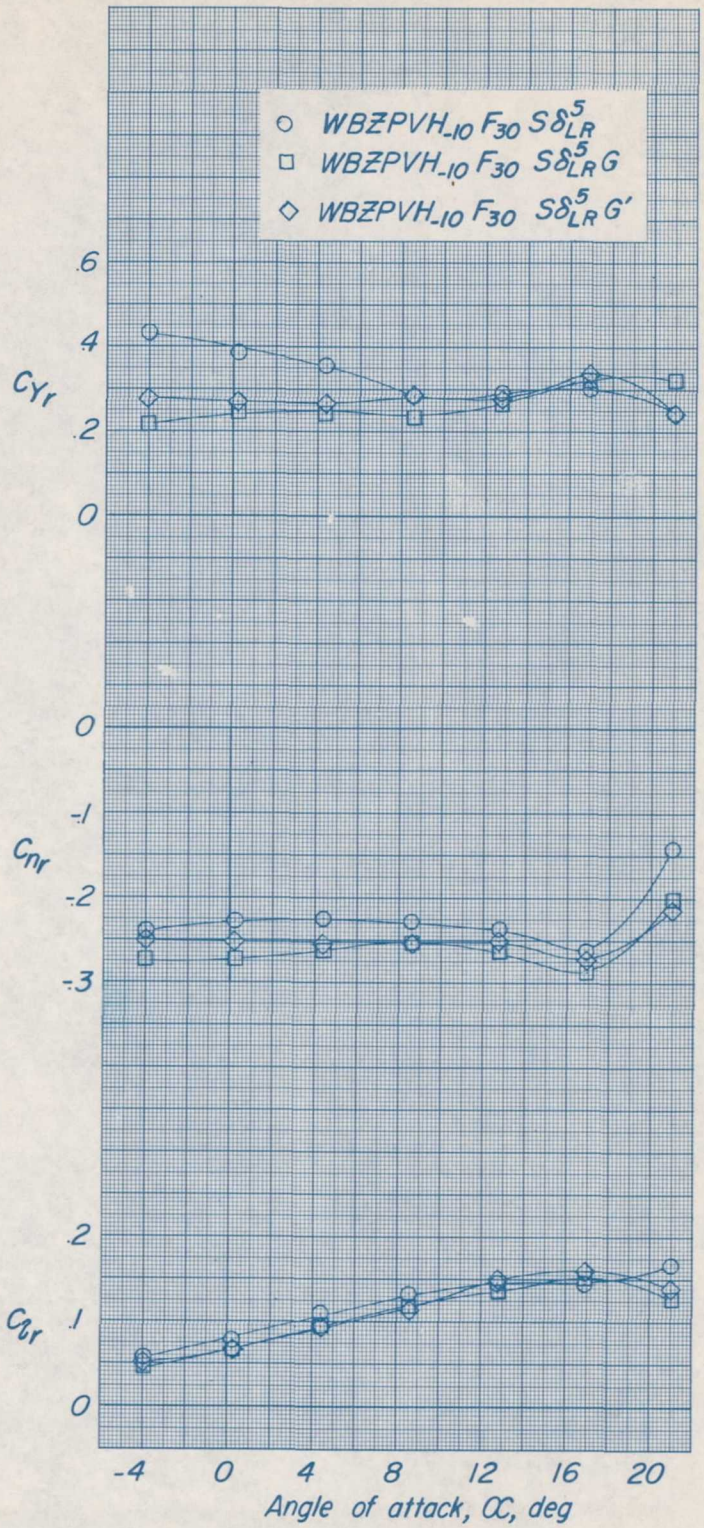

Figure 10.- Effect of landing gear and nose-gear doors on the yawing stability characteristics. Slats, flaps, and flaperons extended.

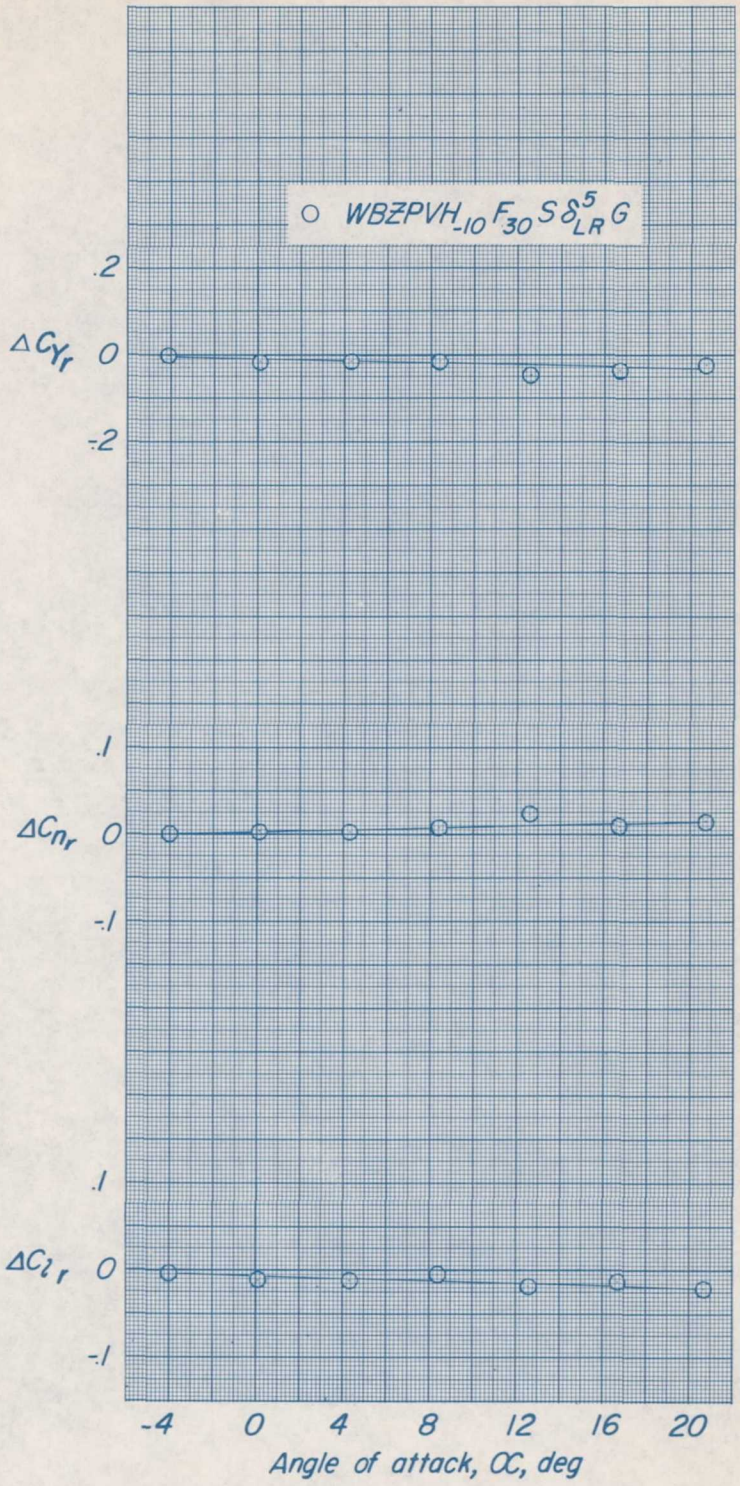

Figure 11.- Support-strut tare increments ΔC_{Y_r}, ΔC_{n_r}, and ΔC_{l_r} plotted against α. Slats, flaps, flaperons, and landing gear extended.

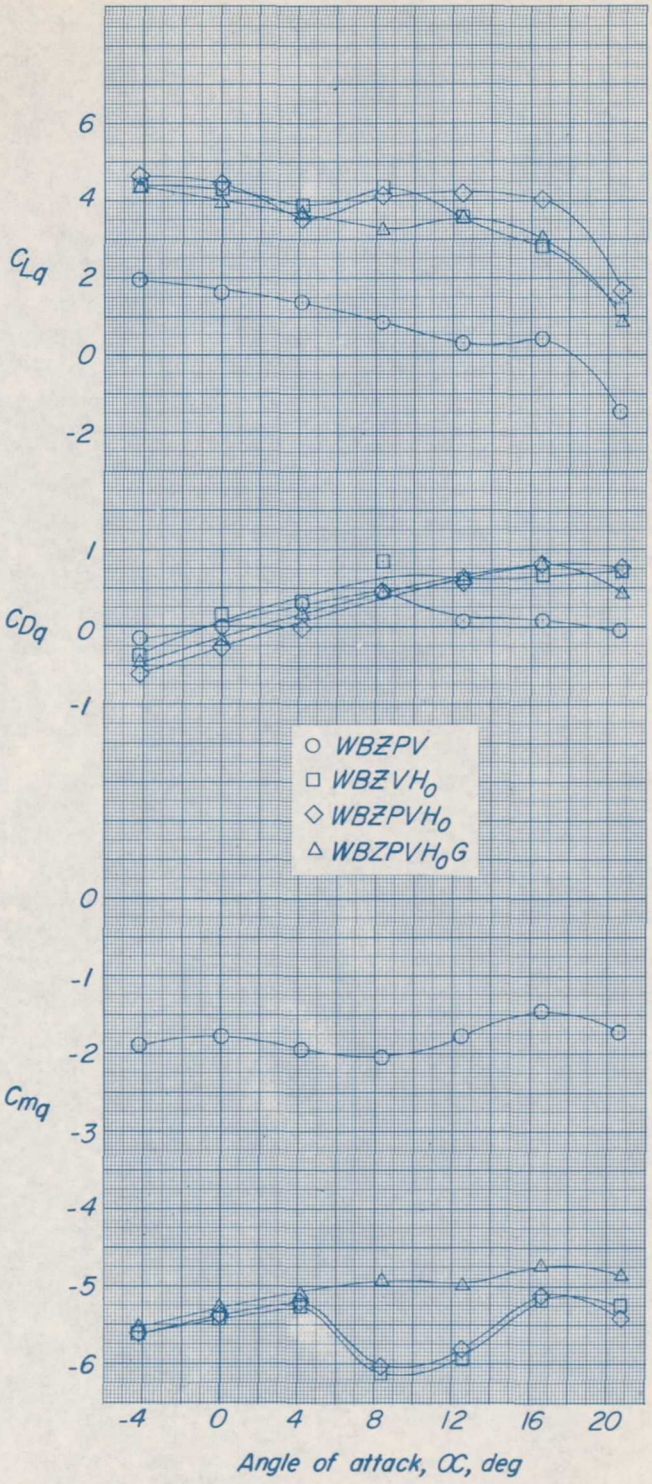

Figure 12.- Horizontal-tail contribution and the effect of duct-entrance-fairing plugs and landing gear on the pitching stability characteristics. Slats, flaps, and flaperons retracted.

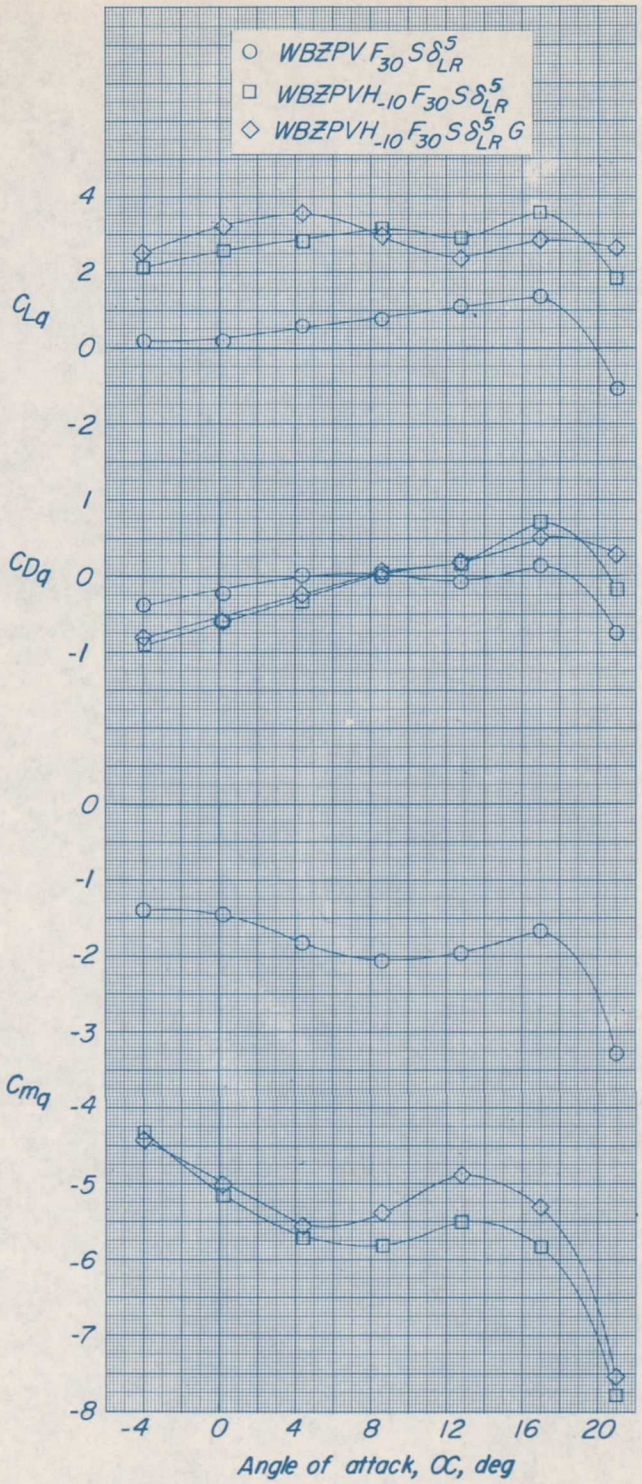

Figure 13.- Horizontal-tail contribution and the effect of landing gear on the pitching stability characteristics. Slats, flaps, and flaperons extended.